Available online at www.sciencedirect.com
SCIENCE DIRECT®
International Journal of Thermal Sciences 44 (2005) 95–105
International Journal of Thermal Sciences
www.elsevier.com/locate/ijts

Performance optimization of solar collector equipped with different arrangements of square-celled honeycomb

A.A. Ghoneim

Applied Sciences Department, College of Technological Studies, P.O. Box 42325, Shuwaikh 70654, Kuwait

Received 10 September 2003; received in revised form 18 March 2004; accepted 24 March 2004

Available online 20 July 2004

Abstract

Honeycomb materials are inserted between the glass cover and the absorber of flat plate solar collector to suppress natural convection. This paper presents the results of an experimental investigation of the thermal performance of solar collector equipped with different arrangements of square-celled honeycomb material. The collector test facility installed at the College of Technological Studies, Kuwait is used to carry out this study. The adapted honeycomb unit is structured from polycarbonate sheet of 10 mm cell size. The effect of air gap thickness above and below the honeycomb material is examined using different arrangements of honeycomb panels with different lenghs. The bottom and top air gap thicknesses are varied from 0 to 12 mm. Experimentally obtained Nusselt number-Rayleigh number plots are presented for free convective heat transfer across honeycomb panels for a wide range of Rayleigh number. Linear regression analysis is implemented to determine the thermal and optical parameters of the solar collector with different honeycomb configurations. A solar collector with air gaps below and above the honeycomb is found to be superior in convection suppression. It is found that the bottom gap thickness is crucial with respect to the heat loss coefficient. The arrangement of honeycomb material with bottom gap thickness of 3 mm is the optimum as it offers the highest efficiency between all arrangements and the lowest heat loss coefficient among other honeycomb configurations. Generally, the results of the present study reveals that compound honeycomb solar collector with proper air gap thickness above and below the honeycomb material attains substantial suppression of free convection.

Keywords: Solar collector; Square-celled honeycomb; Convection suppression; Collector heat losses; Transparent insulation material; Nusselt number; Rayleigh number

1. Introduction

Reduction of heat losses from the absorber to the environment is a major concern for solar collector designers. Selective coatings techniques have been developed to reduce infrared radiation losses from the absorber and in the same time maintain its ability to absorb solar radiation. Higher collector efficiency can be achieved also by using evacuated tube collector. However, manufacturing evacuated tube collector necessitates high technology consequently they are expensive. An interesting alternative to the above mentioned methods can be achieved by inserting a transparent insulation material (TIM) between the plate and the cover of a flat plate solar collector. In this way, both natural convection and radiation heat losses from the top of the absorber can be significantly reduced. Consequently, a flat plate collector equipped with TIM can give performance comparable to vacuum tube collector [1,2]. Honeycomb materials are also adapted to be used in integrated collector storage solar water systems [3].

In early studies honeycomb material is used to completely fill the air gap between the plate and the glazing to suppress convection in flat plate solar collectors. Francia [4] employed circular glass cylinders 15 mm in diameter with length to diameter ratio of 17 to suppress radiative losses from solar collector. Buchberg et al. [5] illustrated the superior performance of a solar collector employing a selectively reflecting rectangular cell honeycomb. Lalude and Buchberg [6] determined the optimum values of design parameters for opaque rectangular honeycombs as well as the design for a honeycomb solar air heater. Buchberg and Edwards [7] investigated the design of cylindrical glass honeycombs which minimize the cost of the collected energy.

E-mail address: aghoneim@paaet.edu.kw (A.A. Ghoneim).

1290-0729/$ – see front matter
doi:10.1016/j.ijthermalsci.2004.03.008

Nomenclature

A	aspect ratio (L/d)		
A_c	collector area	m^2	
c_p	specific heat	$J{\cdot}kg^{-1}{\cdot}K^{-1}$	
D	dimension of squae-celled honeycomb	m	
F_R	heat removal factor		
G	acceleration of gravity	$m^2{\cdot}s^{-1}$	
G	global solar radiation on collector surface	$W{\cdot}m^{-2}$	
h_c	convection heat loss coefficient	$W{\cdot}m^{-2}{\cdot}K^{-1}$	
h_w	wind heat loss coefficient	$W{\cdot}m^{-2}{\cdot}K^{-1}$	
K	thermal conductivity of air	$W{\cdot}m^{-1}{\cdot}K^{-1}$	
L	honeycomb panel height	m	
L_t	total gap thickness	m	
$\dot{m}$	mass flow rate of water	$kg{\cdot}s^{-1}$	
Nu	Nusselt number		
Q_u	rate of useful energy gained	W	
Ra	Rayleigh number		
T_a	ambient air temperature	K	
T_g	glass cover temperature	K	
T_i	inlet fluid temperature	K	
T_o	outlet fluid temperature	K	
T_p	absorber plate temperature	K	
U_L	overall heat loss coefficient	$W{\cdot}m^{-2}{\cdot}K^{-1}$	
v	wind speed	$m{\cdot}s^{-1}$	

Greek symbols

α	thermal diffusivity of air	$m^2{\cdot}s^{-1}$
β	coefficient of volumetric expansion of air	K^{-1}
δ_b	bottom gap thickness	m
δ_t	top gap thickness	m
η	collector efficiency	
ε_g	emissivity of glass cover	
ε_p	emissivity of absorber plate	
ν	kinematic viscosity of air	$m^2{\cdot}s^{-1}$
η	collector efficiency	
θ	collector tilt	deg
σ	Stefan–Boltzman constant	$W{\cdot}m^{-2}{\cdot}K^{-4}$
$(\tau\alpha)_{av}$	average transmittance-absorptance product	

Arnold et al. [8] measured the heat transfer across liquid filled rectangular cell honeycombs with different aspect ratios and tilt angles. Experimental studies carried out by Cane et al. [9] indicated the significant suppression in convection suppression achieved by a thin walled square or hexagonal celled honeycomb even in the inclined position. Smart et al. [10] experimentally determined heat transfer across inclined rectangular honeycomb panels filled with air. The performance of two different collector systems using polycarbonate honeycomb material have been investigated by Rommel and Wagner [1]. Nahar [11] designed a double reflector hot box solar cooker with transparent insulation material (TIM). The energy saving achieved by the use of solar collector with TIM is about 1485 MJ of fuel equivalent by year.

Analytical methods for predicting the efficiency of honeycomb flat plate collectors have indicated significant improvements in performance due to the use of honeycombs [9, 10].

Hollands et al. [12] made experimental and theoretical study of the heat transfer through a solar collector honeycomb. They showed that a separate mode analysis may underestimate the heat flux when selective surfaces are used. A simplified analytical study for the combined mode has been presented by Marcus [13]. Arulanantham and Kaushika [14] studied in detail the combined conduction and radiation heat transfers through transparent honeycomb insulation material. Their study revealed that when either the absorber or the top cover is of the selective type, there is a strong coupling of conductive and radiative heat transfer, therefore a coupled mode analysis must be used to accurately predict the heat transfer. An analytical model for the thermal conductance of double-compound honeycomb transparent insulation has been presented by Hum et al. [15]. Suehrcke et al. [16] developed a numerical model to study heat transfer across honeycomb transparent insulation which showed good agreement with the experimental results.

Slats are also used between the glass cover and the absorber to suppress the fluid motion. Randall et al. [17] presented correlation to calculate the value of the convection suppression with slats. The performance of a flat plate collector with a slatted convection suppression device made of thin glass was investigated experimentally by Charters and Guthrie [18]. Metwally et al. [19] concluded that the thermal performance of flat plate collector with the use of transparent rectangular slats can enhance the efficiency by 34%.

On the other hand, honeycomb materials reduce the collector optical efficiency $(\tau\alpha)$, consequently reduces the thermal performance of the solar collector. Many investigations have been carried out to determine the optical properties of honeycomb structures. Symons [20] measured the solar transmittance of different convection suppression devices using integrating sphere test facility. He presented a correlation for the solar transmittance as function of the incidence angle for honeycomb and various slat geometries. The solar transmittance of different honeycomb structures for incidence angles up to 70° is measured by Platzer [21] using indoor solar simulator and an integrating sphere. Using the individual transmittances of cellular array, Kaushika and Arulanantham [22] developed a model to determine $(\tau\alpha)$ of beam, sky and ground diffuse solar radiations.

To reduce the combined conduction-radiation heat losses from the absorber to honeycomb material, it is necessary

to leave small air gaps above (between honeycomb or slats and glazing) and below (between honeycomb or slats and absorbing plate). This can greatly enhance the thermal performance of solar collectors with honeycomb structure or slats layer in comparison with a similar honeycomb or slats structure without air gaps [23]. Edwards et al. [24] concluded that a honeycomb core will give a good thermal performance for air gaps of 1.5 mm above and or below the honeycomb. A significant decrease in coupled heat transfer across the compound-honeycomb is predicted by Hollands and Iynkaran [25]. This decrease in heat was confirmed in a series of heat transfer measurements made on compound-honeycomb layers with a range of aspect ratios. Abou-Ziyan and Richards [26] experimentally concluded that a compound honeycomb with air gaps above and below the honeycomb significantly enhances the performance of solar collector compared to a compound honeycomb which employs only one air gap below the honeycomb.

The previous discussion indicates the importance of leaving an air gap above and below the honeycomb for decoupling conduction and radiation, thereby reducing heat losses of compound honeycomb collector. Most of the reported work in the literature deals with either heat loss or optical properties, using laboratory measurements. Consequently this treatment separates the honeycomb combined effect of reducing both heat loss and optical efficiency. This may lead to incorrect values of the overall performance of compound honeycomb collector. Thus, the adequate honeycomb thickness and position in the air gap that can suppress convection without reducing the overall collector efficiency needs to be determined using outdoor measurements to determine the collector performance in that case. The present work addresses these issues by investigating the effects of gap thickness on the performance of compound honeycomb collector. The measurements have been made across square-celled honeycomb convection suppressor with a wide range of gap thickness above and below the honeycomb using the solar collector test facility installed at the College of Technological Studies, Kuwait.

2. Experimental setup

A schematic diagram of the collector test facility, designed and constructed to measure the performance of the solar collector is presented in Fig. 1. The collector test facility consists of a solar collector (1), radiation pyranometer (2), storage tank (3) of 100 liters capacity, constant temperature circulator (4), cross flow heat exchanger (5). A centrifugal pump (6) is used to ensure continuous flow of water through the circuit. To permit steam to escape and prevent damage to the system, a pressure relief valve (7) is implemented in the circuit. Also, to allow air to escape from the system, an air vent (8) is adapted at the highest point in the system as shown in the figure. A turbine flowmeter (9) suitable for 0.2 to 5 liters·min^{-1} with accuracy of 3% is used to ensure accurate measurement of fluid flow rate, and a flow control valve (10) is used to adjust the mass flow rate to the

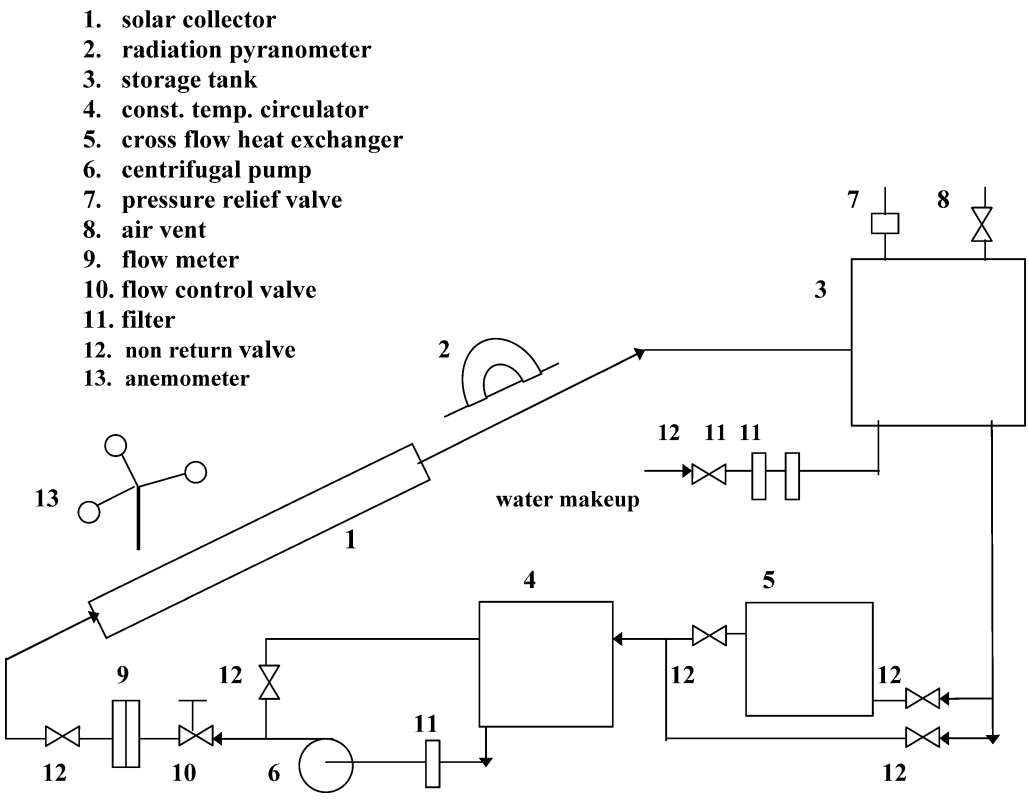

Fig. 1. Schematic diagram of the collector test facility.

value recommended for testing liquid collector. A set of filters (11) and non-return valves (12) are fitted in pipeline to permit flow in one direction. A three cup anemometer with contact closure output (13) is used to measure the wind speed in the vicinity of the collector.

The solar collector designed and manufactured locally has an area of 2 m^2 and an air gap of thickness 60 mm between the absorber plate and the glass cover. The solar collector is mounted on the roof of the main building in the College of Technological Studies, Kuwait and is inclined 30° on the horizontal (Kuwait latitude) facing south. The place of the collector is carefully chosen such that no energy can be reflected on it from any other surfaces and ensuring that shadow will not be cast over the collector at any time during the test period. Eight copper tubes of 12.5 mm outer diameter are distributed and bonded to the absorber plate. These tubes are running between two copper headers made of 42 mm outer diameter tubes. The bottom and sides of the collector are thermally insulated by 15 mm fiber glass followed by 25 mm polystyrene to minimize back and edge heat losses. A clear white, low iron glass sheet of thickness 6 mm is used as a cover.

The absorber is a sheet of copper with thickness 0.5 mm and coated with mat black paint. The absorber is fitted at different positions with ten type-K thermocouples to determine the longitudinal and transversal temperature distribution through the absorber plate. Another thermocouple of the same type is used to measure the glass temperature. The thermocouples are calibrated using a standard platinum resistance thermometer prior to the operation of the collector test. Three standard resistance thermometer detectors (RTD-PT100) are used to monitor the surrounding ambient temperature, inlet and outlet fluid temperatures of the collector. This guarantees high accuracy for these critical temperatures. It is to be noted that the RTD sensor of the ambient temperature is shaded from direct and diffuse solar radiation.

Using closed-loop circuit saves water instead of wasting it as the case in open-loop circuit.The closed-loop circuit is equipped with a storage tank to store hot water outlet from the collector. This hot water is cooled to the desired inlet temperature in two steps. The first step is primary cooling using a cross flow heat exchanger made from finned copper tubes, in the second stage the working fluid is further cooled using a constant temperature circulator. The Haake (model DC50) heating/cooling circulator is capable of supplying up to 12.5 liters·min^{-1} of water at operating temperature ranges from -50 to 200 °C with accuracy of ± 0.01 °C, using a platinum resistance thermometer sensor (PT100) as an input to its controller. The circulator is fitted with standard RS232 interface enabling temperature control through the data acquisition system.

Two Eppley Precision Spectral Pyranometers (PSP model) are used to measure the intensity of the global and diffuse solar radiation incident on the collector surface. One of the pyranometer is mounted in the plane of the collector and at the mid height to measure global radiation. The second one is mounted in the same manner but fitted with a shading ring The pyranometer used to measure the diffuse solar radiation is fitted with a shading ring such that the detector is shielded from direct solar radiation to measure the diffuse radiation only. During tests, the diffuse radiation is assured not to exceed 20% of the total radiation incident on the collector surface during test period ASHRAE Standard [27].

The output of all previously mentioned instruments sensors are connected to a high accuracy data acquisition system (Keithley Model 2700 Multimeter/Data Acquisition) capable of recording 40 channels. The data acquisition system can measure DC voltage to a resolution of 0.1 μV and has a resolution better than 0.01 °C for temperature readings.

3. Square-celled honeycomb panels

The characteristic dimensions of the square-celled honeycomb units as well as their arrangement in the solar collector are shown in Fig. 2. The square-celled honeycomb panels, which is adopted as a convection suppressor, is prepared from polycarbonate sheets (Lexan thermo clear) and it has a row of square cells with a size of 10 mm. The side walls of the honeycomb panel is very thin (about 0.2 mm thick). The spectral radiative transmittance of the honeycomb unit was measured using a spectrophotometer, and the calculated total normal transmittance , reflectance and absorptance for a black body source at 303 K are $\tau = 0.86$, $\rho = 0.07$ and $\alpha = 0.12$. The honeycomb material has a thermal conductivity of 0.35 W·m^{-1}·K^{-1}. The honeycomb panels have a fixed width of 1.0 m (i.e., the same collector width) and a height, L, which is varied during the experiments to obtain the desired bottom (δ_b) and top gap thickness (δ_t). So, the total distance between the absorber and the glass cover (L_t) is given by:

$$L_t = L + \delta_b + \delta_t \tag{1}$$

The panels are packed together using heat sealing then they are installed at right angles to the absorber and the glass cover using wooden spacers. These spacers are prepared specifically for this purpose on a workshop. The spacers are sealed to the absorber plate at different positions using a very thin layer of glue. To ensure the accuracy of the required bottom and top air gap thickness, the wooden spacers thickness was adjusted in the workshop using electronic digital micrometer with a measuring range of 0–25 mm and a resolution of 0.001 mm. The measurements are carried out for this arrangement to determine the performance of the solar collector. Then another sets of panels are prepared but with another height to allow investigation of the solar collector performance over a wide range of bottom and top air gap thickness.

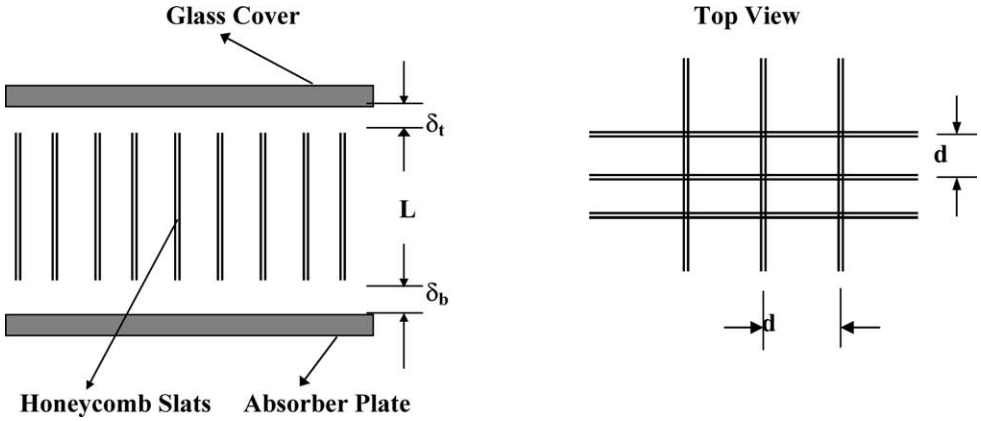

Fig. 2. Square-celled honeycomb dimensions and arrangement in the solar collector.

4. Heat transfer calculations

At steady state conditions, the energy balance equation for the glass cover is given by:

$$h_c(T_p - T_g) + \frac{\sigma(T_p^4 - T_g^4)}{1/\varepsilon_p + 1/\varepsilon_g - 1} = h_w(T_g - T_a) + \sigma\varepsilon_g\left(T_g^4 - T_a^4\right) \quad (2)$$

where h_w is given by:

$$h_w = 5.7 + 3.8v \quad (3)$$

The honeycomb panels are very thin, so the conduction heat transfer through the side walls of the honeycomb panels can be neglected and Nusselt number (Nu) can be expressedd as:

$$Nu = \frac{h_c L_t}{k} \quad (4)$$

The following expression is used to determine Rayleigh number (Ra):

$$Ra = \frac{g\beta(T_p - T_g)L_t^3}{\nu\alpha} \quad (5)$$

For each arrangement of honeycomb panels, measurements of T_p, T_g, T_a, and v were made over a wide range under steady state conditions. In that case, h_c, and Nu can be evaluated from Eqs. (2) and (4), respectively. This procedure are repeated until obtaining Nusselt number over a wide range of Rayleigh number. It should be mentioned that all the fluid properties are calculated at the mean temperature of the absorber and the glass cover.

The measurements are carried out for a certain bottom and top gap thickness using wooden spacers to determine Nu as function of Ra. Then another sets of panels are configured and prepared but with another height to allow calculations at different top and bottom air gap thickness. The characteristics of the different cases studied are listed in Table 1. Uncertainty in the measured Rayleigh number, resulting from the uncertainty in total gap thickness, plate temperature, and glass cover temperature is estimated to be ±3%. The uncertainty in measured Nusselt number, resulting from the uncertainty in total gap thickness, plate temperature, glass cover temperature, ambient temperature, and wind speed is estimated to be ±4%.

Table 1
Gap characteristics of the cases studied

Case no.	δ_b [mm]	δ_t [mm]	L [mm]	% δ_b/L_t	% δ_t/L_t
1	0	0	60	0.0	0.0
2	0	3	57	0.0	5.0
3	3	0	57	5.0	0.0
4	6	0	54	0.0	10.0
5	3	3	54	10.0	0.0
6	3	6	54	5.0	5.0
7	6	3	51	5.0	10.0
8	3	9	51	10.0	5.0
9	3	12	48	5.0	15.0
10	6	6	48	10.0	10.0

5. Measurements of collector performance

A number of initial tests have been performed to examine the durability and reliability of the collector against extreme weather conditions. These tests are static pressure test, high temperature stagnation test, thermal shock/water spray test and collector time constant test. Such tests are performed according to the certification of operation issued by Florida Solar Energy Center [28]. The results of these tests confirmed the durability and reliability of the manufactured collector. It should be noted that the collector is not stagnation proof as the honeycombs start melting at 120 °C [1].

The performance of the flat plate solar collector without honeycomb panels is determined first. Then, the performance of the solar collector with different arrangements of honeycomb panels is investigated. Tests performed include different arrangements of bottom and top air gap thickness. The characteristics of the different cases studied are listed in Table 1.

The tests are carried out for global solar radiation between 600 and 1000 $W{\cdot}m^{-2}$, on a 30° tilted collector surface with average ambient temperatures from 30 to 41 °C.

The inlet water temperature is changed from around the ambient up to 90 in 10 °C steps.

The experimental procedure is started by flushing the system. Then, the system is filled with water and the flow rate is adjusted to the required value. The predetermined inlet fluid temperature is fixed using the cross flow heat exchanger and the constant temperature circulator. The solar collector is allowed to run for about 1 h (about 10 times the collector time constant) to achieve quasi-steady-state conditions before the data collections were started. The data acquisition system records all readings of ambient, fluid and plate temperatures, flow rate, and global and diffuse solar intensity every minute. Each experiment continued for 2 h after that the inlet fluid temperature is changed and a new experiment is started until the set of runs is completed for this arrangement. It should be mentioned that the experiments are performed before noon and repeated again after noon to provide similarity around the solar noon. This would minimize the collector heat capacity effect [29]. The measurements for each arrangement are allowed to run for one week to ensure that data contains reasonable number of quasi-steady state conditions. Then, the collector cover is removed and another case is implemented and tested.

A FORTRAN computer program is written to extract the points that represent quasi-steady state conditions from measurements according to the recommendations advised by ASHRAE, 1986. This is confirmed by the fact that, within the test period of 15 min (more than twice the collector time constant), the maximum variations in ambient, inlet and outlet temperatures are ±0.5 °C, ±0.2 °C and ±0.2 °C, respectively, while in global radiation is ±20 $W{\cdot}m^{-2}$. Also, the diffuse radiation is assured not to exceed 15% of the global radiation in any experiment. The accepted data for each test period are averaged and used in the analysis as a single point, while other data are rejected. The above discussion revealed that the data presented here comply with the requirements outlined in ASHRAE Standard [27].

Using heat balance equation and knowing the inlet and outlet fluid temperatures, the mass flow rate of water and the total incident radiation, the thermal efficiency (η) of a solar collector at steady state can be evaluated from the following equation:

$$\eta = \frac{Q_u}{A_c G} = \frac{\dot{m} c_p (T_o - T_i)}{A_c G} \tag{6}$$

According to Duffie and Beckman (1991), the thermal efficiency (η) of a solar collector at steady state conditions can be also calculated using one of the following efficiency equations:

$$\eta = F_R\left[(\tau\alpha)_{\text{av}} - U_L(T_i - T_a)/G\right] \tag{7}$$

$$\eta = (\tau\alpha)_{\text{av}} - U_L(T_p - T_a)/G \tag{8}$$

Eq. (7) is commonly used to present collector performance since measurement of inlet fluid temperature (T_i) is usually more easier than measurement of mean plate temperature (T_p). On the other hand, using Eq. (8) directly predicts the optical efficiency $(\tau\alpha)_{\text{av}}$ and the total heat loss coefficient (U_L). For this reason, it was decided to present the data using Eq. (8) in the present study. The experimental results are presented in forms of graphs and equations that describe the collector efficiency against a reduced temperature parameter $(T_p - T_a)/G$.

The uncertainty analysis shows an experimental error of about 0.8, 1.4 and 3.2% for U_L, $(\tau\alpha)_{\text{av}}$, and the collector efficiency, η, respectively. The uncertainty analysis, for the experimental data fitted by Eq. (8), revealed that the optical efficiency, $(\tau\alpha)_{\text{av}}$, is more sensitive to experimental error than the heat loss coefficient, U_L.

6. Results and discussions

6.1. Heat transfer calculations

To check the reliability of the present measurements as well as the procedure followed in predicting *Ra* and *Nu*, the measurements are carried out first for a solar collector with the air gap is completely filled with honeycomb panels (i.e., $L = L_t = 60$ mm). The aspect ratio, A, which is defined as the ratio of honeycomb height (L) and honeycomb cell dimension (d) in this case is equal to 6. The measurements are compared with the correlation proposed by Cane et al. [9] for square-celled honeycomb. They proposed the following correlation for Nusselt number (*Nu*) as function of Rayleigh number (*Ra*):

$$Nu = 1 + 0.89\cos\left(\theta - \frac{\pi}{3}\right)\left(\frac{Ra}{2420A^4}\right)^{2.88-1.64\sin\theta} \tag{9}$$

It should be noted that Eq. (9) is valid for the range:

$$\frac{Ra}{A^4} \leqslant 6000, \quad 30^\circ \leqslant \theta \leqslant 90^\circ, \quad A \geqslant 4 \tag{10}$$

The present measurements are found to agree well with Cane et al. [9] correlation which confirms the reliability and accuracy of the present measurements.

Fig. 3 presents the plot of Nusselt number versus Rayleigh number for only some of the cases studied for the sake of clearity. As seen from the figure, there are two limiting cases: an air layer, and the case corresponding to $\delta_b = \delta_t = 3$ mm. These two cases give upper and lower limits of convective heat transfer in the combound honeycomb collector studied. The *Nu–Ra* plot shows two distinctly different shapes characterized by the gradual rise and the abrupt rise. For air layer, natural convection starts at the well-known critical Rayleigh number ($Ra_c = 1.7 \times 10^3$), then the Nusselt number rises rapidly. For the other limiting case ($\delta_b = \delta_t = 3$ mm), the Nusselt number remains very close to unity until a critical value of Rayleigh number, $Ra_c = 3.6 \times 10^5$, is reached after which it rises gradually with Rayleigh number over the measurement range. This second limiting case ($\delta_b = \delta_t = 3$ mm) gives the best performance, i.e., the lowest Nusselt number and consequently the lowest heat transfer coefficient.

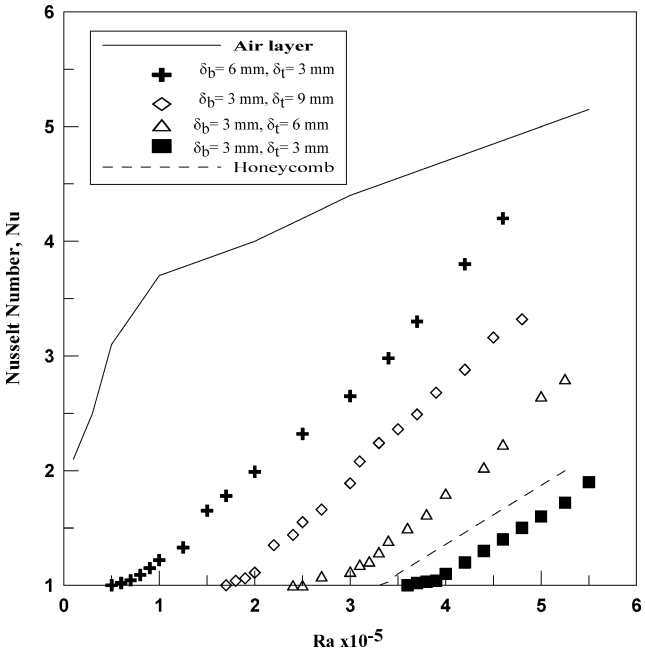

Fig. 3. Experimental results for Nusselt number-Rayleigh number for different honeycomb configurations.

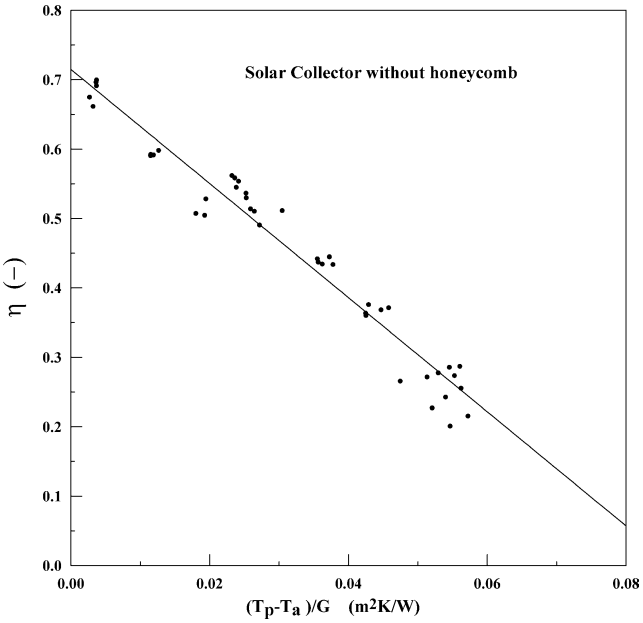

Fig. 4. Efficiency versus $(T_p - T_a)/G$ for solar collector without honeycomb.

As the thickness of air gaps above and below the square celled honeycomb is further increased, the critical Rayleigh number for the compound collector decreases. Increasing the thickness of air gaps reduces the importance of honeycomb in suppressing convection. In addition increasing the gap thickness raises the critical valueof Rayleigh number. As seen from the figure, the bottom gap thickness is more significant than the top gap thickness. A bottom gap thickness of 3 mm and top gap of 9 mm can still gives a performance better than the case of case ($\delta_b = 6$ mm, $\delta_t = 3$ mm). For the case giving the lowest heat transfer ($\delta_b = \delta_t = 3$ mm), the total air gap is 10% of the total spacing between the absorber plate and the glass cover.

It is interesting to mention that it is found that for bottom gap thickness greater than 9 mm and at some Rayleigh number, the effect of honeycomb can increase not decrease the heat transfer over that which would occur for the case without honeycomb.

6.2. Thermal performance of solar collector

To judge the effect of honeycomb material, the solar collector is tested first with no honeycomb in place. Fig. 4 presents the variations of collector efficiency versus the reduced temperature parameters $(T_p - T_a)/G$. The average points of the experimental data are shown in the figure. The scatter of the data around the straight line is mainly attributed to the angle of incidence variations, wind speed and the dependence of U_L on the plate temperature. Also, the variations of the relative proportions of beam, diffuse and ground reflective components of solar radiation are participating in the data scattering. Thus, scatters in the data are to be expected, however, it is acceptable that collectors are characterized by the line intercept $(\tau\alpha)_{\text{av}}$ and the slope, which is the total heat loss coefficient (U_L).

The experimental data are fitted with linear equations to provide the characteristic parameters of the collector in order to compare it with those of the compound honeycomb collector. The efficiency is expressed by the following equation with R^2 of 0.973.

$$\eta = 0.72 - 8.21(T_p - T_a)/G \tag{11}$$

Comparing the above equation with Eq. (8) gives optical efficienct $(\tau\alpha)_{\text{av}} = 0.72$ and heat loss coefficient $U_L = 8.21$. It should be noted that this tested collector has no selective coating for absorber or antireflective coating for glass cover.

6.3. Performance of solar collector with honeycomb panels

The performance of the compound honeycomb solar collector is tested for various gaps thickness above and below the honeycomb. The characteristics of the cases studied are presented in Table 1. Fig. 5 shows the test results for some of the tested cases for simplicity purpose. The scatters in the data are observed again because of U_L temperature dependence, wind effects and angle of incidence variations. However the scatters in the data for honeycomb panels are lower than that for solar collector without honeycomb. This is because U_L is less dependent on temperature in cases of honeycomb panels.

The data are fitted with linear regression and the intercepts and slopes of the linear equations are presented in Table 2 for the cases studied. Table 2 reveals that the intercepts $(\tau\alpha)_{\text{av}}$ vary from 0.60 to 0.64. The transmissivity of

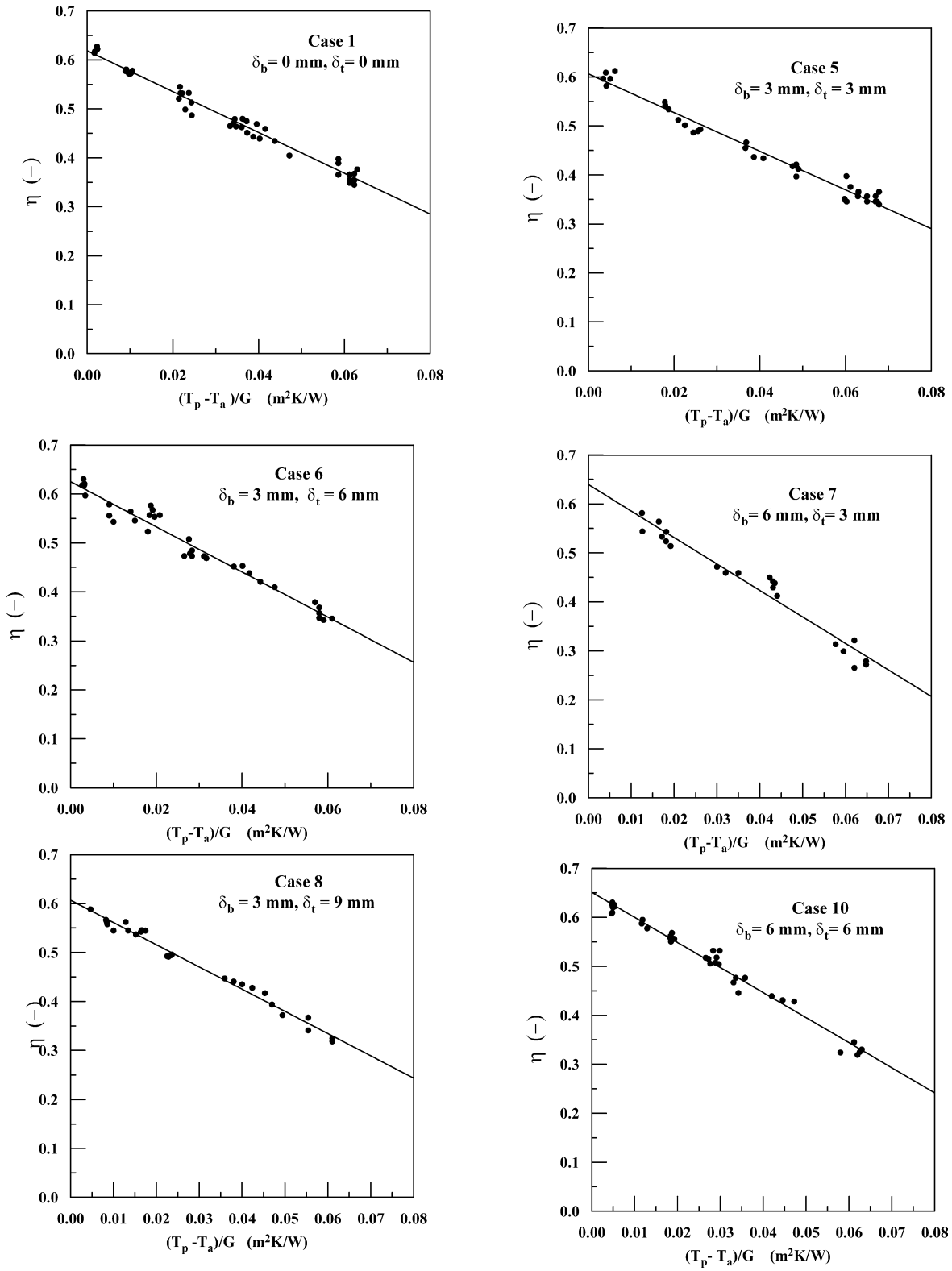

Fig. 5. Efficiency versus $(T_p - T_a)/G$ for honeycomb cases (different gap thickness).

compound collector is independent on the position of the honeycomb in the gap. Thus these small variations may be attributed to data scattering. Also the changes of top and bottom gaps may have altar radiation shape factor slightly. However, the average value of $(\tau\alpha)_{av}$ can be considered as 0.62 ± 0.02 indicating very small discrepancy in the results.

The values of U_L, listed in Table 2, change from 3.91 to 5.38 (about 38%) as the bottom gap changes from 0 to

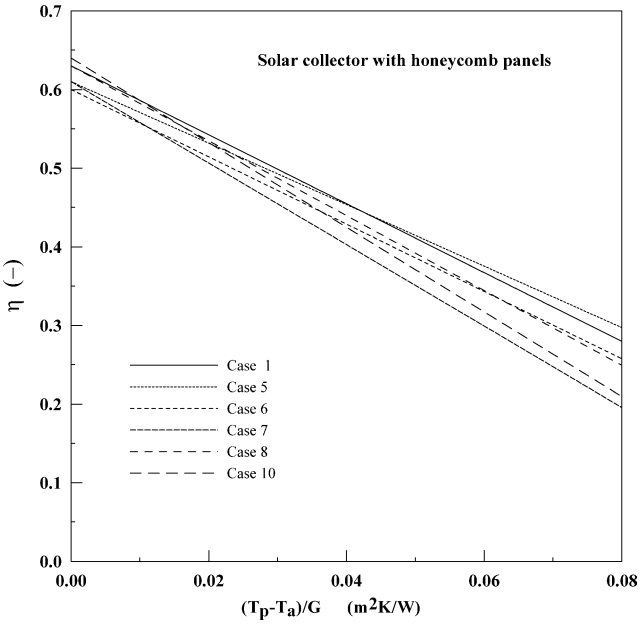

Fig. 6. Effect of gap thickness on the collector efficiency for honeycomb cases.

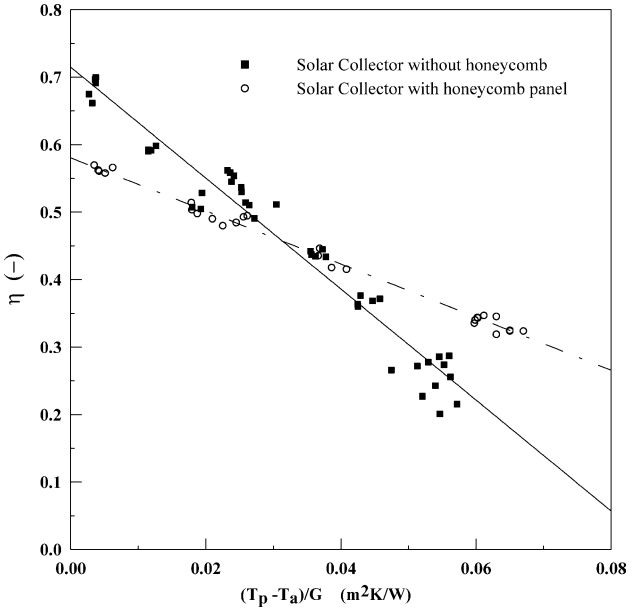

Fig. 7. Comparison between best compound collector case and solar collector without honeycomb.

Table 2
Characteristic parameters of solar collector equipped with honeycomb panels

Case no.	δ_b [mm]	δ_t [mm]	$(\tau\alpha)$	U_L [W·m^{-2}·K^{-1}]	R^2
1	0	0	0.63	4.38	0.981
2	0	3	0.62	4.22	0.987
3	3	0	0.61	4.43	0.994
4	6	0	0.64	4.85	0.984
5	3	3	0.61	3.91	0.976
6	3	6	0.60	4.28	0.965
7	6	3	0.61	5.18	0.958
8	3	9	0.63	4.76	0.986
9	3	12	0.62	5.04	0.952
10	6	6	0.64	5.38	0.988

12 mm. This indicates the strong dependence of U_L on the position of the honeycomb in the air gap. However, it is to be expected that bottom gap thickness would have greater effect for collectors of selective surfaces.

Fig. 6 presents the efficiencies of some tested cases of compound honeycomb collector against $(T_p - T_a)/G$. For the sake of clarity, only the linear regression equations (reported above) of the test results are presented in the figure. Since, the variations in $(\tau\alpha)_{\text{av}}$ are small, the efficiency curves are close at low values of reduced temperature parameter. As this parameter increases the curves diverge because the efficiency becomes more dependent on $F_R U_L$. Thus the curves are ordered according to the values of the heat loss coefficient. Clearly, case 5 ($\delta_b = 3$ mm, $\delta_t = 3$ mm) produces the highest collector performance whereas case 10 ($\delta_b = 6$ mm, $\delta_t = 6$ mm) gives the lowest performance. This indicates the strong effect of gap thickness on the performance of compound honeycomb collector.

The results presented in Fig. 6 reveals that there is an optimum gap thickness around 3 mm. This can be explained in the light of the heat transfer mechanism in the compound honeycomb collector. As the bottom gap thickness approaches zero, the conduction from absorber plate to honeycomb walls increases and consequently radiation from the relatively warm honeycomb walls becomes significant. This results in increase in U_L compared to that occurred at the optimum gap thickness. On the other side, if the bottom gap is increased beyond the optimum thickness, convection from absorber to honeycomb walls increases causing radiation from honeycomb to increase. Thus, the optimum gap thickness must be attempted in order to attain heat loss coefficients at low values and achieve proper design of the honeycomb and collector.

The effect of bottom gap thickness on U_L can be more evaluated by relating the values for compound honeycomb collector to that for the solar collector without honeycomb. The last point on the curve presents the solar collector without honeycomb. Clearly, at the optimum bottom gap thickness (3 mm), the value of U_L can be reduced by about 48%, if proper design of compound honeycomb collector is achieved, compared to solar collector without honeycomb. This shows the significant improvement accomplished when using compound honeycomb collector with proper configuration.

6.4. Comparison between solar and compound honeycomb collectors

In order to conclude the effect of honeycomb panels on the collector performance, the arrangement that produced the best performance among all cases are compared with reference to the solar collector without honeycomb. Fig. 7

shows the efficiency variations with reduced temperature parameter for case 5 and for collector without honeycomb. The solar collector without honeycomb has a higher value of $(\tau\alpha)$. The compound honeycomb collector reduces the optical efficiency $(\tau\alpha)$ by about 14%. On the other hand, the collector without honeycomb produces much higher heat loss coefficient. The reduction in the heat loss coefficients for collectors using honeycomb panel compared to collector without honeycomb is 52%. The honeycomb acts to reduce both heat loss coefficient (U_L) and the optical efficiency $(\tau\alpha)$. The combined effect of these two factors changes the intercept and slope of the efficiency curves. The effect of optical efficiency is dominant at low temperature difference whereas the effect of heat loss is important at high temperature difference. Thus, the efficiency of compound honeycomb collector is better than that without honeycomb particularly at medium and high temperatures. On the other hand, the collector without honeycomb gives better efficiency for limited low temperature range.

Fig. 7 shows an intersection between the efficiency curves for the collector without honeycomb and the collector with honeycomb panel at reduced temperature parameter of 0.026. This proves that good design of compound honeycomb collector has obvious enhancement over that for the collector without honeycomb in the practical range of reduced temperature parameter.

7. Conclusions

A solar collector equipped with square-celled honeycomb panels of different arrangements is investigated. The experimental data are analyzed and the performance resulted from the regression analysis are reported for different arrangements. Based on the experimental results, the following conclusions can be drawn:

- The use of honeycomb in solar collectors has the benefit of reducing the top heat loss and also the penalty of decreasing the optical efficiency. Thus unless proper design of honeycomb is accomplished, honeycomb may deteriorates the collector performance. Apart from honeycomb material and aspect ratios, the proper design involves adequate length of honeycomb and appropriate gap thickness above and below the honeycomb.
- Free convection heat transfer across an air layer can be effectively suppressed by a thin walled square-celled honeycomb.
- Bottom gap thickness value is more crucial than top gap thickness in suppressing convective heat transfer.
- Significant reduction in heal loss coefficient (U_L) value can be accomplished for collector that uses honeycomb panels with proper value of air gap thickness.
- The reduction in optical efficiency $(\tau\alpha)$ for collector that uses honeycomb panels is insignificant compared to the reduction achieved in heal loss coefficient (U_L).

Acknowledgements

The author wish to thank Kuwait Foundation for the Advancement of Sciences (KFAS) for its financial support of the research under the project no. (02-10-99).

References

[1] M. Rommel, A. Wagner, Application of transparent insulation materials in improved flat plate collectors and integrated collector storage, Solar Energy 49 (1992) 371–380.
[2] A. Goetzberger, M. Rommel, Prospects for integrated storage collector systems in Central Europe, Solar Energy 39 (1987) 211–219.
[3] K.S. Reddy, N.D. Kaushika, Comparative study of transparent insulation materials cover systems for integrated collector storage solar water heaters, Solar Energy Materials & Solar Cells 58 (1999) 431–446.
[4] G.A. Francia, A new collector of solar radiant energy-theory and experimental verification, in: United Nations Conference on New Sources of Energy, Rome, Italy, 1961.
[5] H. Buchberg, O.A. Lalude, D.K. Edwards, Performance characteristics of rectangular honeycomb solar thermal converters, Solar Energy 13 (1971) 193–221.
[6] O.A. Lalude, H. Buchberg, Design of honeycomb porous bed solar air heaters, Solar Energy 13 (1971) 223–242.
[7] H. Buchberg, D.K. Edwards, Design considerations for solar collectors with cylindrical glass honeycombs, Solar Energy 18 (1976) 193–203.
[8] J.N. Arnold, I. Catton, D.K. Edwards, Experimental investigation of natural convection in inclined rectangular regions of different aspect ratio, J. Heat Transfer 98 (1976) 67–71.
[9] R.L.D. Cane, K.G.T. Hollands, G.D. Raithby, T.E. Unny, Free convection heat transfer across inclined honeycomb panels, J. Heat Transfer 99 (1977) 86–91.
[10] D.R. Smart, K.G.T. Hollands, G.D. Raithby, Free convection heat transfer across rectangular celled diathermanous honeycombs, J. Heat Transfer 102 (1980) 75–80.
[11] N.M. Nahar, Design. Development and testing of a double reflector hot box solar cooker with a transparent insulation material, Renewable Energy 23 (2001) 167–179.
[12] K.G.T. Hollands, G.D. Raithby, F.B. Russell, Wilkinson, Methods for reducing heat losses from flat plate solar collectors, Report No. COO-2597-5, University of Waterloo, 1979.
[13] S.L. Marcus, An approximate method for calculating the heat flux through a solar collector honeycomb, Solar Energy 30 (1983) 127–131.
[14] M. Arulanantham, N.D. Kaushika, Coupled radiative and conductive thermal transfers across transparent honeycomb insulation materials, Appl. Thermal Engrg. 16 (1996) 209–217.
[15] E.Y. Hum, K.G.T. Hollands, J.L. Wright, Analytical model for the thermal conductance of double-compound honeycomb transparent insulation, with validation, Solar Energy 76 (2003) 85–91.
[16] H. Suehrcke, D. Däldehög, J.A. Harris, R.W. Lowe, Heat transfer across corrugated sheets and honeycomb transparent insulation, Solar Energy 76 (2003) 351–358.
[17] K.R. Randall, J.W. Mitchell, M.M. El-Wakil, Natural Convection Characteristics of Flat Plate Collectors, Heat Transfer in Solar Energy Systems, American Society of Mechanical Engineers, New York, 1977.
[18] W.W.S. Charters, K.I. Guthrie, Experimental evaluation of slatted convection suppression devices, in: Solar World Forum, vol. 1, Pergamon Press, Oxford, 1982, pp. 181–185.
[19] M.N. Metwally, H.Z. Abou-Ziyan, A.M. El-Leathy, Performance of advanced corrugated-duct solar air collector compared with five conventional designs, Renewable Energy 10 (1997) 519–537.

[20] J.G. Symons, Calculation of the transmittance-absorptance product for flat plate collector with convection suppression device, Solar Energy 33 (1984) 637.
[21] W.J. Platzer, Directional-hemispherical solar transmittance data for plastic honeycomb-type, Solar Energy 49 (1992) 359–369.
[22] N.D. Kaushika, M. Arulanantham, Transmittance-absorptance product of solar glazing with transparent insulation materials, Solar Energy Materials & Solar Cells 44 (1996) 383–395.
[23] N.D. Kaushika, K. Sumathy, Solar transparent insulation materials: A review, Renewable & Sustainable Energy Reviews 37 (2003) 317–351.
[24] D.K. Edwards, J.N. Arnold, I. Catton, End-clearance effects on rectangular-honeycomb solar collectors, Solar Energy 18 (1976) 253–257.
[25] K.G.T. Hollands, K. Iynkaran, Analytical model for the thermal conductance of compound honeycomb transparent insulation, experimental validation, Solar Energy 51 (1993) 223–227.
[26] H.Z. Abou-Ziyan, R.F. Richards, Effect of gap thickness on a rectangular–cell compound-honeycomb solar collector, Solar Energy 60 (1997) 271–280.
[27] ASHRAE, ASHRAE Standard 93-86, Methods of Testing to Determine the Thermal Performance of Solar Collectors, Atlanta, Georgia, USA, 1986.
[28] Florida Solar Energy Center, Operation of the Collector Certification Program, FSEC-GP-6-80, Cocoa, Florida 32922-5703, 2002.
[29] J.A. Duffie, W.A. Beckman, Solar Engineering of Thermal Process, Wiley–Interscience, New York, 1991.